scientific reports

Check for updates

OPEN

Cow dung waste as an eco-friendly adsorbent for Alizarin Red S dye removal

Ali El-Rayyes[1,2], Abidemi Mercy Babatimehin[3,4]✉, Moamen S. Refat[5], Amnah Mohammed Alsuhaibani[6], Akeem Adesina Bamigbade[7], Nathanael Yinka Ilesanmi[3] & Edwin Andrew Ofudje[3]

In this study, cow dung waste (CDW), acid-treated cow dung waste (ATCDW), and base-treated cow dung waste (BTCDW) were evaluated for the removal of Alizarin Red S (ARS) from aqueous solutions using UV–Vis spectroscopy. The adsorbents were characterized using Fourier Transform Infrared Spectroscopy (FT-IR), Scanning Electron Microscopy with Energy Dispersive X-ray Spectroscopy (SEM-EDX), and X-ray Diffraction (XRD) to understand their structural and surface properties. The adsorption optimal conditions for the adsorption of ARS were obtained as ARS concentration of 300 mg/L, pH of 2, temperature of 45 °C, and contact time of 100 min for CDW and ATCDW, 80 min for BTCDW respectively. The adsorption isotherms indicated that CDW and ATCDW followed the Freundlich model, suggesting a heterogeneous adsorption process, while the adsorption of ARS by BTCDW adhered to the Langmuir model, indicative of monolayer adsorption. The maximum adsorption capacities, calculated from the Langmuir model, were 58.24 mg/g for CDW, 87.54 mg/g for ATCDW, and 61.37 mg/g for BTCDW at 45 °C. Kinetic studies revealed that the adsorption of ARS onto CDW and ATCDW followed the pseudo-second-order model, while BTCDW adsorption was best described by the pseudo-first-order model. Thermodynamic analysis showed that the adsorption process was endothermic, with enthalpy values of 48.12 kJ/mol for CDW, 95.22 kJ/mol for ATCDW, and 7.55 kJ/mol for BTCDW. FT-IR analysis confirmed the presence of functional groups such as O–H, C=O, and C–O, which are associated with cellulose, hemicellulose, and lignin, facilitating dye interactions through electrostatic forces. These results suggest that cow dung waste, especially when treated, is a promising, cost-effective, and eco-friendly adsorbent for the removal of organic contaminants like ARS from wastewater.

Keywords Adsorption, Cow dung, Dyes, Optimization, Water

Pollution of the environment due to rapid industrialization is of major concern to environmentalists due to the danger it posed to man, and it environs[1]. Hazardous substances from industries such as paints, pharmaceuticals, electroplating, textiles, plastic, and paint contains dye components which pollute water bodies such as ponds, lakes, seas and reservoirs with underground water not been left out of this menace[2,3]. Though dyes are colorful materials which are often used to add to the aesthetics of mater, their presence in water bodies often in forms of effluents render the water useless even when they are present at low concentration[2–4]. Synthetic dyes are widely used in industries such as printing, textiles, cosmetics, and leather, with Alizarin Red S (ARS) being one of the salient anthraquinone-based dyes. ARS is a water-soluble dye commonly used for dyeing silk, wool, and biological staining[5,6]. However, when discharged into aquatic environs via poorly treated or untreated industrial effluents, it poses serious health and environmental risks. ARS is known for its chemical stability and resistance to biodegradation, making it persistent in water bodies where it can disrupt photosynthesis, reduce light penetration, and exhibit toxic effects on aquatic life[7,8]. In humans, exposure to ARS has been reported to

[1]Center for Scientific Research and Entrepreneurship, Northern Border University, 73213 Arar, Saudi Arabia. [2]Chemistry Department, College of Science, Northern Border University, Arar, Saudi Arabia. [3]Department of Chemical Sciences, Mountain Top University, Pakuro, Ogun State, Nigeria. [4]Department of Biochemistry, Lagos State University, Ojo, Lagos, Nigeria. [5]Department of Chemistry, College of Science, Taif University, P.O. Box 11099, Taif 21944, Saudi Arabia. [6]Department of Sports Health, College of Sport Sciences & Physical Activity, Princess Nourah bint Abdulrahman University, P.O. Box 84428, Riyadh 11671, Saudi Arabia. [7]Department of Chemistry, College of Physical Sciences, Federal University of Agriculture, Abeokuta, Ogun State, Nigeria. ✉email: abidemibabatimehin530@gmail.com

be associated with allergic dermatitis, eye and skin irritation, respiratory disorders, and potential mutagenic and carcinogenic effects[9–11].

It thus becomes very imperative to research into their elimination from wastewater and the environment. Consequently, the removal of dyes is essential prior to discharging effluents into natural waterways, making it a prominent focus in contemporary material and environmental research. In the past years, several physicochemical and biological technologies have been explored for eliminating synthetic dyes like ARS from wastewater. Some of these methods are membrane filtration, coagulation-flocculation, photodegradation, chemical oxidation, adsorption, ion-exchange, and biological treatment[12–16]. Although effective to some extent, some of these techniques suffer from notable setbacks such as chemical oxidation and coagulation often results in the production of harmful byproducts or toxic sludge, others like membrane technologies is often faced with issues like high operational costs and fouling[17,18]. Biological methods on the other hand, though environmentally friendly, may be ineffective for non-biodegradable dyes like ARS and often require long treatment times. These limitations underscore the need for the search for alternative, cost-effective, and sustainable approaches to dye removal[9–11].

Among available treatment technologies, adsorption has gained considerable interest because of its simplicity, low energy requirements, high efficiency, and adaptability to a wide range of contaminants[10,11,19]. In low-income regions like Nigeria, the application of activated carbon as an adsorbent is most times limited, because of its high cost and regeneration issues. In this context, the use of animal wastes and agricultural as low-cost adsorbents has emerged as a promising alternative. In adsorption processes, commercial activated carbon is the most utilized adsorbent because of its bigger surface area, but its high cost has often limited its usage especially by household[4]. This had resulted in research into the use of other forms of adsorbents which are readily available and cheap for the uptake of pollutants from aqueous solutions. Dumping waste of agricultural origin inform of trash in the environs is a usual practice in developing countries like Nigeria and this often constitute nuisance in the environment and in most case, they are washed into river body by erosion. However, research focusing on the utilization of waste agricultural products as effective adsorbent for wastewater treated as an alternative to commercial activated carbon have been documented in literature and some of such waste's materials are rice husk[20], fish bones[21], pig bones[22], eggshells[23], crab shells[24], poultry litter[25], cow manure[26].

Cow dung wastes are excreted food materials by cattle which is made up of hemicellulose, urine and feces, cellulose, and lignin[27]. Rapid increase in cattle business due to high demand of beef and dairy milk production had resulted in the released of large amount of dung waste into the environment constituting public health challenge. For instance, it was reported that Nigeria's milk generation in 1972 rose from 229,000 metric tons to 700,000 metric tons in 2021[28]. Additionally, the report projected that in the next five years, the dairy industrial production in the country is expected to grow by 6.56%, reaching $27 billion by 2028[28]. Thus, with projected increase in the value chain of cattle business, it's equally expected that waste generation from it will be on the rise and there must be deliberate attempt to find a means of not only eliminating from the environment but also transforming them to meaningful product like adsorbent. To the best of our knowledge, cow dung waste and its treated forms have not been documented in the literature for the uptake of ARS molecules from contaminated wastewater and this we intend to exploit. Although the use of agricultural and animal waste for environmental remediation has gained attention in recent years, the potential of cow dung as a low-cost, eco-friendly adsorbent remains significantly underexplored, particularly for the removal of synthetic dyes such as Alizarin Red S (ARS). While preliminary studies suggest that cow dung possesses surface-active functional groups capable of adsorbing various contaminants, there is a limited understanding of the specific adsorption mechanisms involved in the interaction between cow dung and ARS molecules. Detailed molecular-level insights, is still lacking. Furthermore, there is a pressing need to examine how modification or treatment of cow dung such as acid or base treatment, can enhance its adsorption efficiency and stability. Current studies often use raw cow dung, which may contain impurities or pathogens, yet little has been done to explore how pre-treatment can improve both adsorption capacity and safety. Another major gap is the lack of research on the regeneration and reusability of cow dung-based adsorbents particularly for the removal of synthetic dyes such as Alizarin Red S (ARS. Without sustainable regeneration methods, the application of cow dung may result in secondary waste issues, undermining its environmental advantages.

In view of the above, we utilized cow dung as an adsorbent for the elimination of ARS dye. The effect of factors like dye concentration, contact time, cow-dung waste (CDW), temperature and pH on the reaction process was investigated. Different structural studies as well as various kinetics and isotherm models were deployed to describe the dye removal mechanism by the adsorbent.

Experimentation

Materials

Cow dung waste adsorbent preparation

Cow dung materials were collected from Cattle Ranch in Ogun State, Nigeria and cleansed with distilled water severally to eliminate odour. The obtained product was sun dried for fifteen days before grinding them and subsequently sieved them to obtain fine particles. The samples were divided into three portions with one portion treated with a 0.1 M HCl and labeled as acid-treated cow dung waste (ATCDW), the second part treated with 0.1 M NaOH is labeled as base-treated cow dung waste (BTCDW) while the third portion was used without further treatment and referred to as cow dung waste (CDW). After treatment, distilled water was used to were washed the samples until neutral pH.

Characterizations

The structural analysis of the adsorbent was carried out using various techniques. Surface imaging was done via Scanning Electron Microscopy (SEM-EDX; EVO MA-10, Carl Zeiss, Jena, Germany). FT-IR spectra were

obtained by an FT-IR spectrometer to identify surface functional groups, within 4000 to 400 cm^{-1} range at 4 cm^{-1} resolution (Bruker Tensor 27 spectrophotometer). X-ray diffraction (XRD) test was done on an X'PERT Pro PANalytical diffractometer with a Cu Kα radiation source. Peaks were recorded at 2θ values ranging from 5° to 65°, with a step size of 0.013. The zeta potential was determined using a Zetasizer Nano ZS (Malvern, UK). Before determination, 0.1 mg of the sample was finely ground and dispersed in distilled water to enhance light scattering for accurate zeta potential analysis. The dispersion was then sonicated for 15 min to break up particle agglomerates and achieve uniform distribution. Surface area and pore size distribution were evaluated via Brunauer–Emmett–Teller (BET) analysis, done with a NOVA 4000e BET instrument (Quantachrome Corporation, Anton Paar USA).

Preparation of ARS solution and batch adsorption process

The Alizarin Red S also known as sodium alizarin sulfonate (Diadema, Brazil, 95% purity) with structure shown in Fig. 1 was used without further purification. The ARS stock solution was prepared by dissolving suitable amount of ARS into deionized water in standard flask. Other solutions used were made from the stock solution above via serial dilution with distilled deionized water to get the required ARS concentration. From the prepared solution of ARS, 25 ml was withdrawn into a beaker, followed by pH regulation with dilute solution of either 0.1 M HNO_3 or NaOH Thereafter, 0.4 g of CDW was introduced into the beaker containing ARS solutions and agitated on an orbital shaker. At different time, aliquot amount of ARS for was taken for analysis using an UV–visible spectrophotometer model V-570 after filtration. The adsorption process was reaped trice, and the average values were reported. The procedure was adopted to study the effect of other factors and the adsorbed amount of ARS (Q_e) in mg/g and the percentage removal (%R) were obtained using the equations below:

$$Q_e = \frac{C_o - C_e}{m} \times v \tag{1}$$

$$\%R = \frac{C_o - C_e}{C_o} \times 100 \tag{2}$$

With C_o and C_e denoting ARS initial and supernatant concentration in mg L^{-1} respectively. While ARS volume in L is denoted by V and CDW mass used is given as m in g. The experiments were conducted in triplicate and the average value was recorded. The range of parameters evaluated are temperature of 25 to 65 °C, reaction time of 20 to 140 min, ARS concentration of 50 to 300 mg/L, pH of 2 to 6, and adsorbent dosage of 0.1 to 1 g.

Regeneration evaluation

Regeneration experiments were done after each adsorption cycle, desorption was performed using acetic acid to remove the adsorbed Alizarin Red S. The adsorbent was subsequently washed, dried, and reused in successive adsorption cycles to assess its long-term stability. Following desorption, the mixture was separated,

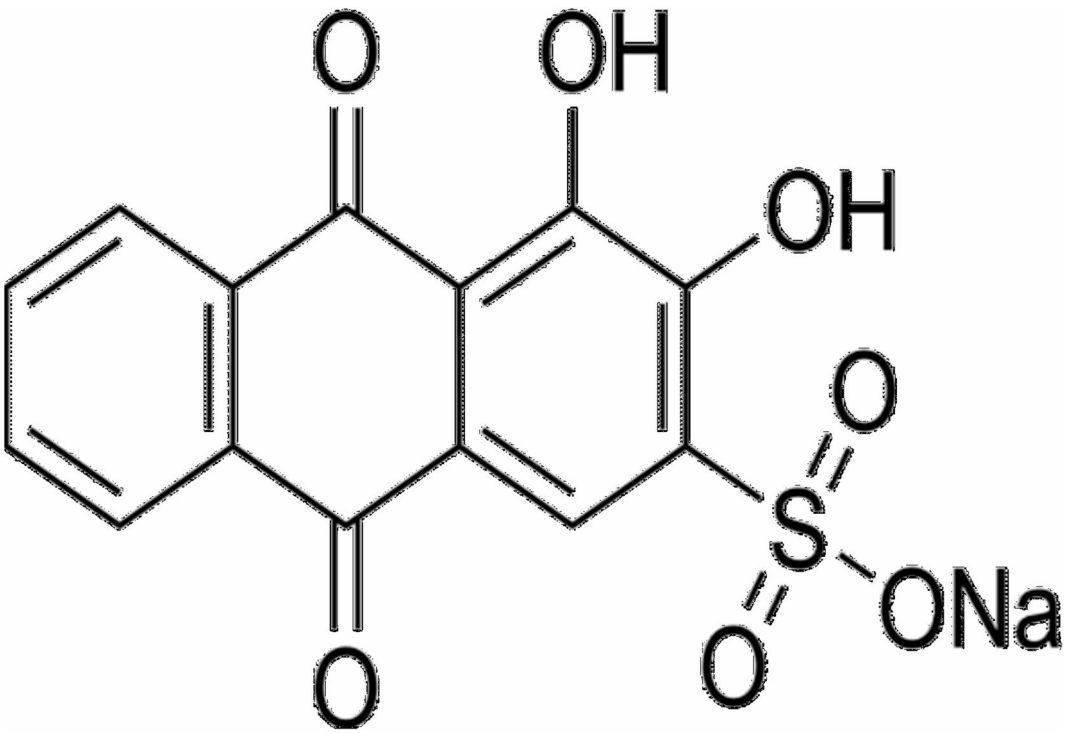

Fig. 1. Structure of Alizarin red S.

and the remaining Alizarin Red S content was analyzed using UV-visible spectrophotometer model V-570. This procedure was repeated in five cycles following same protocol, and the percentage desorption (PD) was calculated using Eq. (3) provided below.

$$PD(\%) = \frac{AD}{AA} \times 100 \tag{3}$$

where AD is the amount of Alizarin Red S desorbed (mg), and AA is amount adsorbed (mg).

Results and discussions

Characterizations

The comparison of cow dung waste (CDW), acid-treated cow dung waste (ATCDW), and base-treated cow dung waste (BTCDW) underscores the significant impact of chemical treatment on key sorption properties, including surface area, pore volume, and pore size. The surface area increased from 62.4 m^2/g for CDW to 85.5 m^2/g for BTCDW, and further to 94.2 m^2/g for ATCDW. A similar trend was observed in pore volume, with values rising from 0.35 cm^2/g (CDW) to 0.44 cm^2/g (BTCDW) and 0.62 cm^2/g (ATCDW). These enhancements indicate improved porosity in the treated samples, which in turn boosts their adsorptive potential. Moreover, the average pore size of the chemically treated samples was larger than that of the raw CDW, suggesting that acid and base treatments induce structural modifications that increase accessibility for adsorbate molecules. TThe SEM images illustrates the morphological evolution of cow dung under various conditions, including before and after adsorption, as well as following acid and base treatments as shown in Fig. 2. In image (a), depicts raw cow dung before adsorption, the surface appears relatively smooth and compact, with embedded irregular particles. This structure indicates limited porosity and fewer active sites available for adsorption. After adsorption, as seen in image (b), the image shows a noticeable increase in surface irregularity, with fibrous and flake-like structures emerging. These changes indicate that the adsorbate has reacted with the adsorbent and likely altered the surface.

Figure 2c, which shows acid-treated cow dung before adsorption, shows a much more porous and fractured structure. The treatment seems to have removed some mineral or organic content, thereby increasing surface area and opening up the pores. Upon adsorption, image (d) reveals that some of the pores appear to be filled or blocked, indicating successful uptake of adsorbate. In image (e), which shows the base-treated cow dung before adsorption, fragmented and granular texture which is much distinct from both untreated and acid-treated samples were seen. This implies that the base treatment likely caused disintegration of structural components, thereby increasing the surface accessibility of the adsorbent. In image (f), that depicts the base-treated cow dung after adsorption, the surface appears denser, with signs of material deposition on the surface. This suggests that adsorption has occurred, with adsorbate occupying available pores on the surface. In all, the SEM images confirm that both acid and base treatments enhance the surface behaviour of cow dung material, making it more effective as an adsorbent. Acid treatment appears to have produce deeper crevices and well-defined porous structures, whereas base treatment results in a more fragmented and granular morphology.

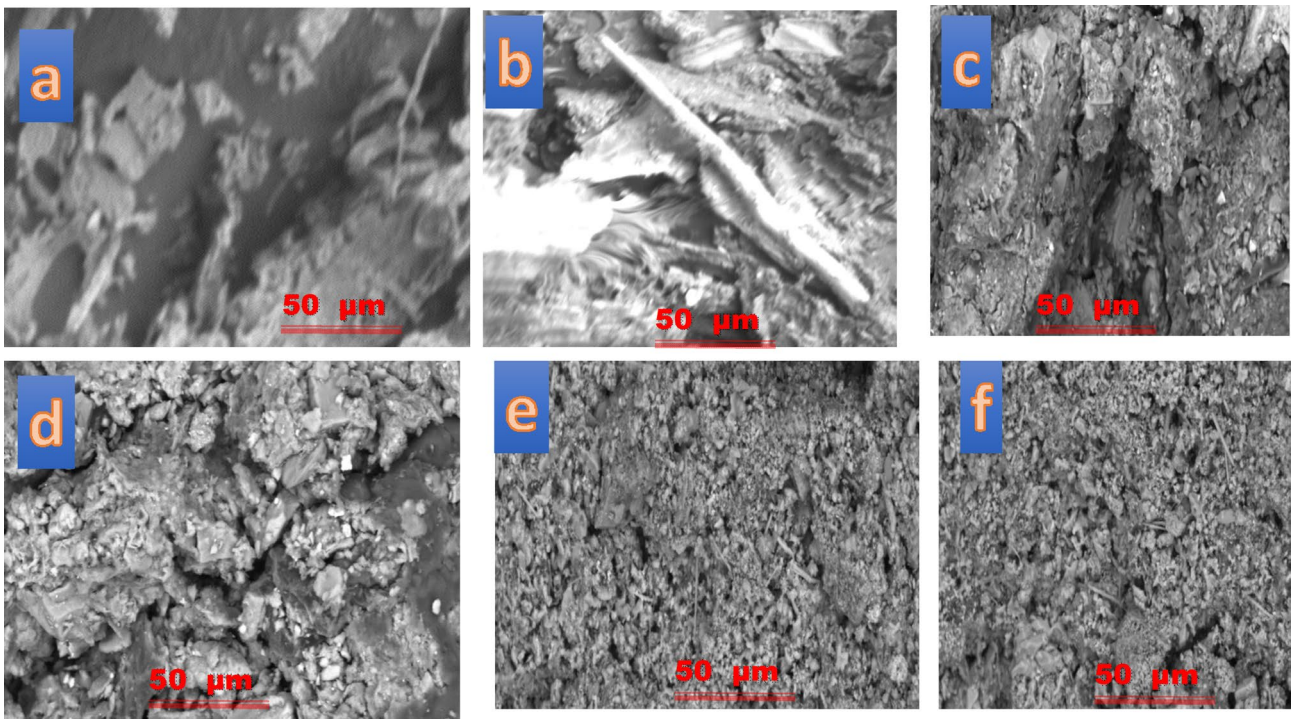

Fig. 2. CDW images (**a**) before and (**b**) after the uptake of ARS.

FT-IR scan of cow dung waste before and after ARS dye adsorption was done and the results obtained are as provided in Fig. 3. The cow dung waste spectrum before adsorption, the observed peak at 3280.06 cm^{-1} is due to O–H stretching from cellulose and lignin, while the peaks at 2855.14 cm^{-1} and 2922.23 cm^{-1} are peculiar to C–H bands, typical of methylene and methyl groups in cellulose and hemicellulose[29–31]. The triple bond stretching from alkynes, C≡C or C≡N stretching, possibly from nitriles was seen at 2102.22 cm^{-1}. The band at 1636.30 cm^{-1} is assigned to C=O bond in amides or C=C bond in alkenes, which could be linked to proteins (amide I band) or unsaturated fatty acids. The band at 1563.55 cm^{-1} relates to N–H bending (amide II) in proteins or aromatic ring vibrations. The peak at 1423.85 cm^{-1} arising from C–H bending (CH_2), suggests the presence of fatty acids or lipids, while the peak at 1375.39 cm^{-1} represents C–H bending (CH_3), indicating the presence of aliphatic hydrocarbons or methoxy groups in organic matter[32–34]. The band at 1319.59 cm^{-1} relates to C–N bond or O–H bending vibrations, often seen in amines or carboxylic acids, suggesting the presence of proteins or amino acids in the dung. The C–O stretching vibrations peak is seen at 1036.20 cm^{-1}, which could arise from carbohydrates (cellulose, hemicellulose) or other organic substances like lignin[32–34]. The FT-IR spectrum reveals significant peaks related to carbohydrates (cellulose, hemicellulose), proteins, lipids, and possibly some organic acids. The existence of N–H, O–H, C–O, C–N, C=O, and C–H bonds reflects the complex mixture of biological materials in cow dung, including plant matter, proteins, and fats. The peaks also indicate the presence of fatty acids and water content, which are typical components of cow dung. The peaks related to N–H, O–H, C=O, C–O and aromatic rings suggest that the dye interacts with cow dung. For example, the peak observed at 3280.06 cm^{-1} shifted to 3198.06 cm^{-1}, indicating interactions between the O–H or N–H groups in cow dung and the O–H groups of Alizarin Red S (ARS), likely through hydrogen bonding or chelate formation. The peak at 1997.85 cm^{-1} may represent overtone or combination bands of carbonyl or aromatic groups. Since ARS, an anthraquinone dye, contains C=O bonds and an aromatic system, this peak could result from interactions between cow dung and the dye, potentially from ARS's carbonyl or aromatic overtones. The peak originally at

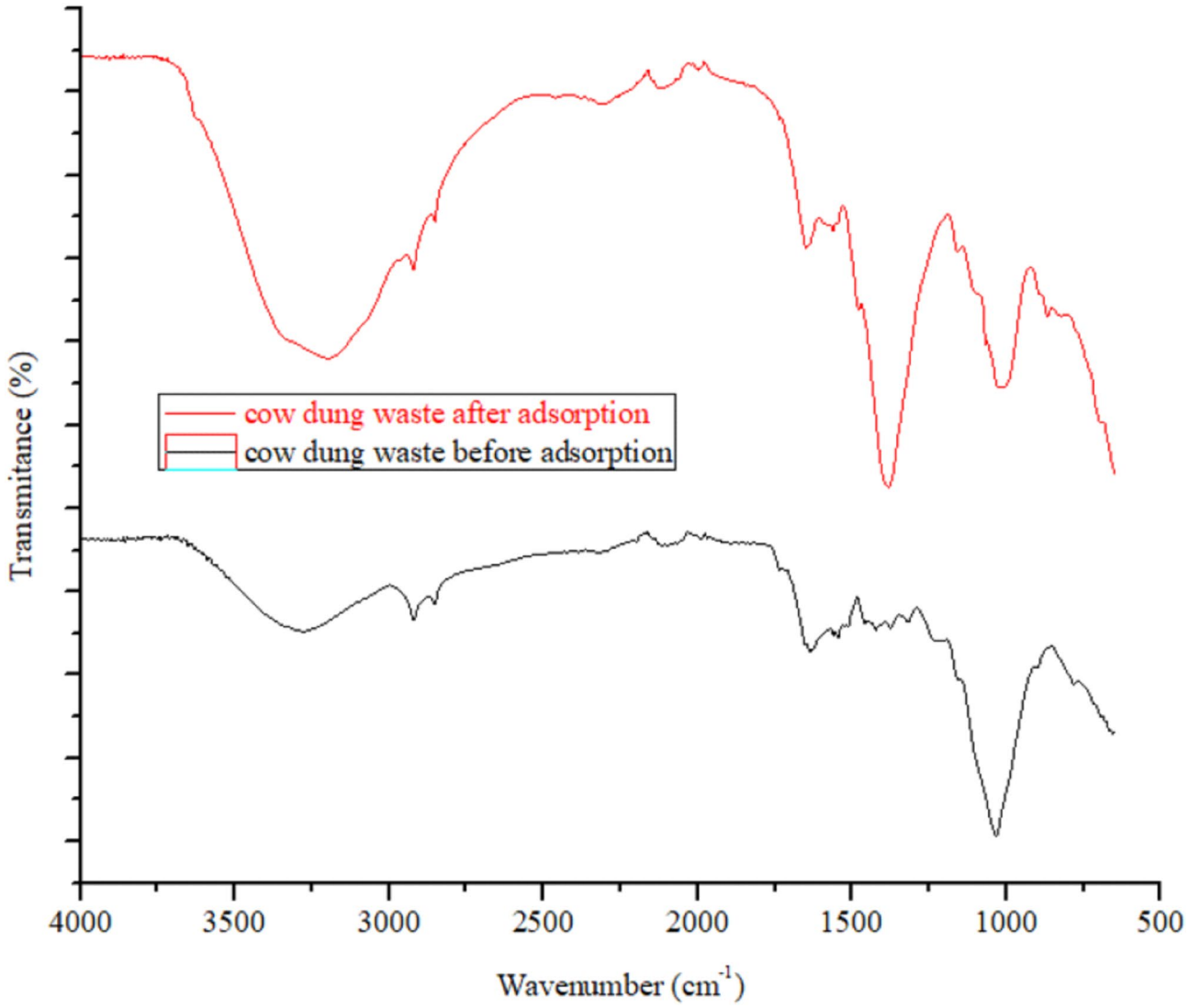

Fig. 3. FT-IR of cow dung before and after adsorption of ARS.

1636.30 cm^{-1} before interaction with ARS shifted to 1651.21 cm^{-1}, which suggests interactions between cow dung's organic components, such as proteins, and the dye's carbonyl groups. The N–H bending (amide II) or aromatic ring vibrations observed at 1563.55 cm^{-1} shifted to 1558.03 cm^{-1}, indicating possible interactions between ARS's aromatic rings and proteins or aromatic compounds in cow dung. Similarly, the C–O stretching peak at 1036.20 cm^{-1} in cow dung before ARS adsorption shifted to 1006.38 cm^{-1} after adsorption, indicating structural changes in the carbohydrate of cow dung due to interaction with ARS molecules. The new band seen at 868.47 cm^{-1} relates to aromatic compounds C–H out-of-plane bending, especially in substituted benzenes or aromatic systems. This peak likely reflects interactions with aromatic or phenolic compounds in cow dung, possibly through π–π interactions, as ARS has an aromatic structure. Overall, the FT-IR spectrum also indicates that cow dung interacts with ARS mainly through hydrogen bonding and possible metal ion coordination.

The patterns of cow dung waste XRD before and after ARS uptake are shown in Fig. 4. The XRD pattern of cow dung before adsorption was observed at 21° which is associated with semi-crystalline structure of cellulose from undigested plant material since cellulose is a key structural component in plants, and cow dung typically contains partially digested or undigested plant fibers[35]. After the adsorption of ARS, no visible changes occurred suggesting that the adsorption of ARS by the cow dung adsorbents do not have any effect on the bulk crystalline structure of the adsorbent which could be attributed to the fact the uptake of the ARS molecules occurred on the surface of the adsorbent and not within the the internal crystal structure. The elemental composition of the cow dung is shown in Fig. 5 which revealed the presence of O (56.59%), Ti (2.11%), Na (24.81%) and C (16.49%).

pH effect on the adsorption of ARS

The adsorbents' adsorption capacity significantly influenced by the concentration of hydrogen ions in the solution. For this work, the pH of the ARS solution was varied from 2.0 to 6.0, as shown in Fig. 6. When the pH was fixed at 2.0, the capacity of adsorption for the three adsorbents tested was at its highest, with the acid-treated biomass demonstrating the most effective pollutant removal. The CDW, ATCDW, and BTCDW adsorption

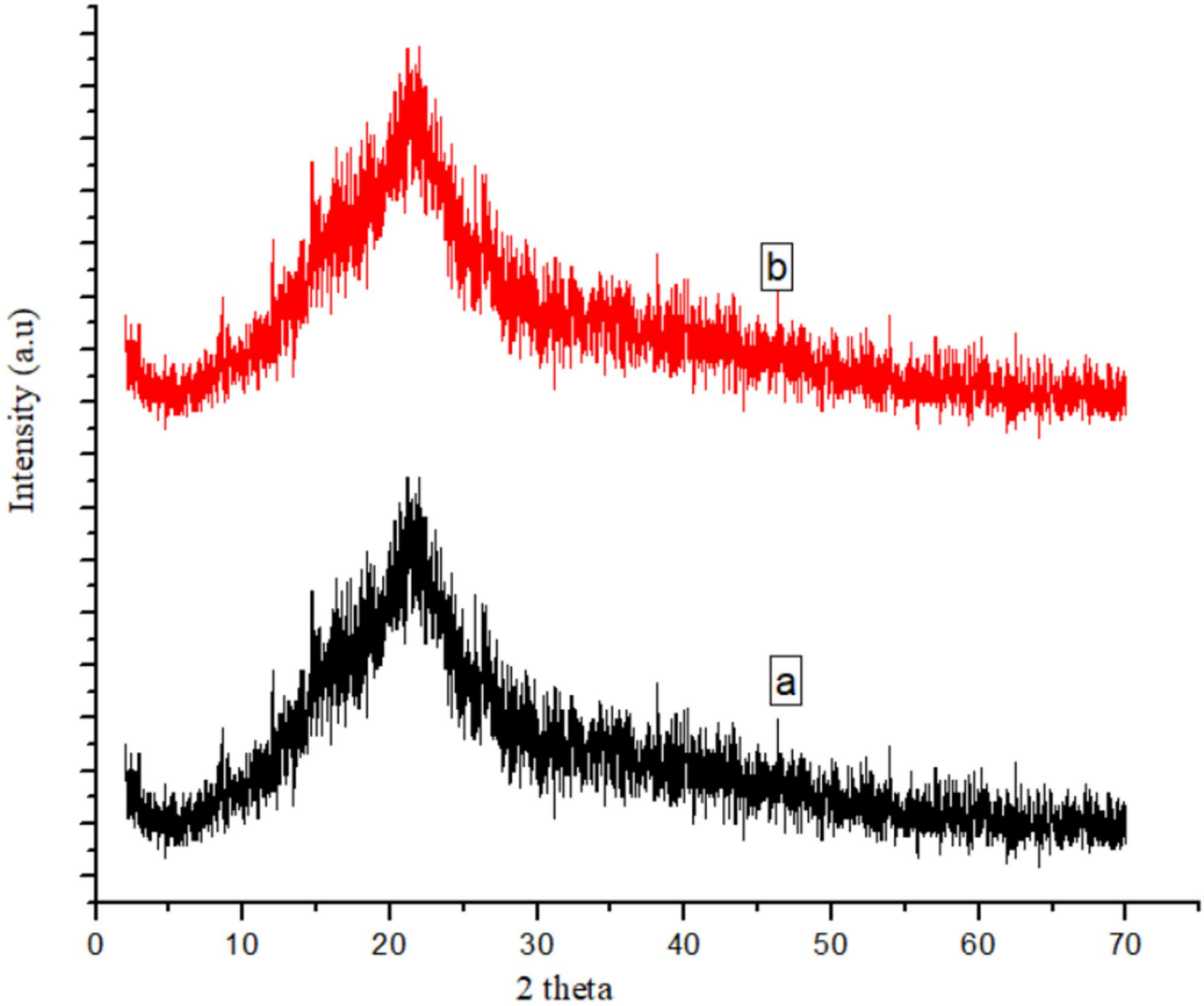

Fig. 4. XRD of cow dung (**a**) before and (**b**) after adsorption of ARS.

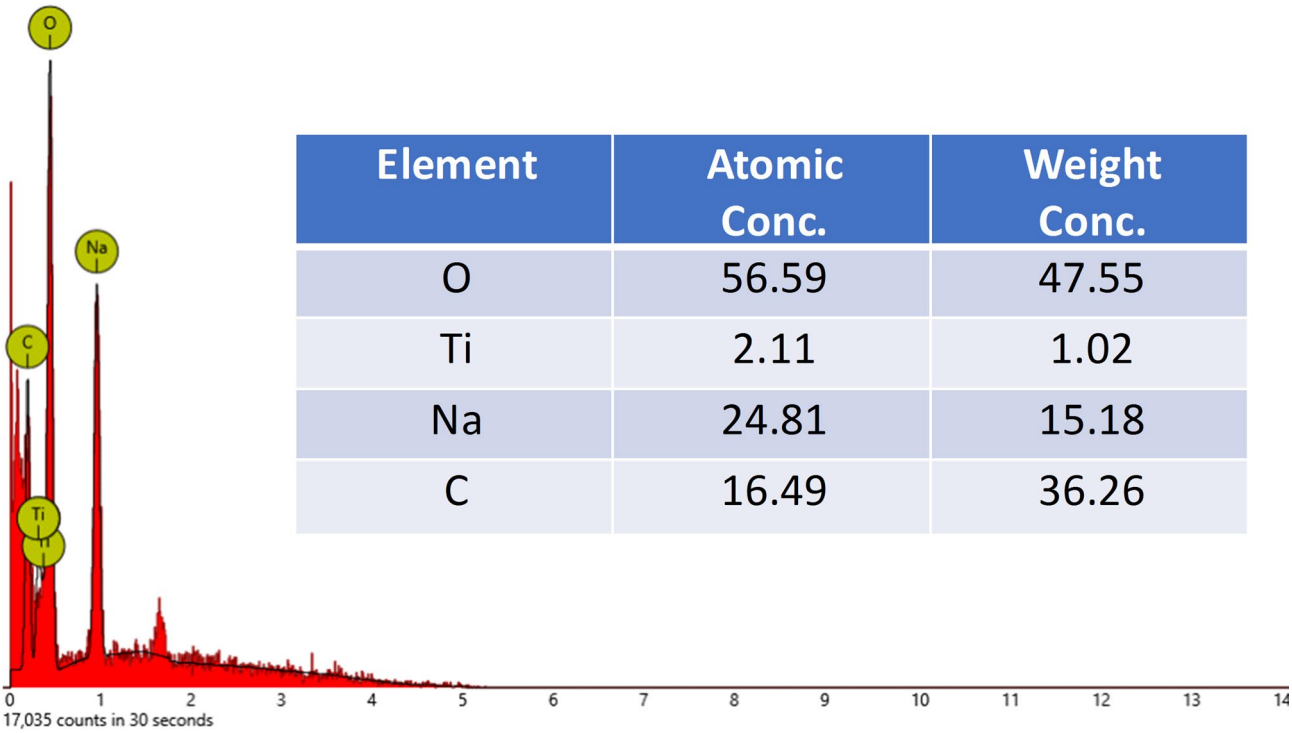

Element	Atomic Conc.	Weight Conc.
O	56.59	47.55
Ti	2.11	1.02
Na	24.81	15.18
C	16.49	36.26

Fig. 5. Elemental compositions of cow dung waste.

potency decreased from 67.82 to 54.32%, 86.45–65.33%, and 82.37–60.32%, respectively, on adjusting the pH of ARS from 2.0 to 6.0. The enhanced adsorption at lower pH values could be because of the protonation of the adsorbent's receptive groups and the anionic nature of the ARS dye. It has been reported that these receptive groups are highly acidic, with negative pKa values, which allows for the uptake of the dye through the positively charged adsorbent surface at pH of 2.0, and facilitated by electrostatic attraction[11,36]. Experiment on zero-point charge (pHpzc) were conducted to further assess the impact of pH on the sorption process and the estimated values are 5.2, 4.2, and 5.6, for CDW, ATCDW, and BTCDW respectively. It is expected that at pH values lower than these pHpzc values, the cow dung waste surface will be positively charged[5,36]. At pH values lower than the pHpzc (5.2, 4.2, and 5.6 for CDW, ATCDW, and BTCDW), the adsorbent surfaces will be positively charged, enhancing electrostatic attraction between the positively charged adsorbent surface and the anionic ARS molecules, leading to higher adsorption efficiency. Conversely, as the pH increases (from 2.0 to 6.0), the adsorbent surface becomes less positively charged and eventually negatively charged (above the pHpzc), which weakens the electrostatic interaction with the negatively charged ARS molecules. This explains the decrease in adsorption capacity as the pH increases, as shown in the experimental results. At pH 6.0, the adsorbents' surfaces are more negatively charged, and fewer electrostatic interactions occur between the adsorbent and the anionic ARS molecules, resulting in a significant reduction in adsorption. In the adsorption of of alizarin Red S biosorption by *Alhagi maurorum as reported by* Akram et al.[37], it was observed that at acidic values of pH (3.0 to 6.0), the biosorbent surface is likely to positively charged, and that this enhance the interaction between the biosorbent and the ARS dye molecules that are negatively charged. However, with the pH rising above pH 6, the biosorbent surface became negative resulting into electrostatic repulsion between the biosorbent surface and ARS molecules, causing reduction in the removal percentage.

Effect of adsorbent amount

The role played by the various adsorbents amount on ARS removal was studied. Figure 7 shows the plots of the various amount of the adsorbent on the eradication of ARS, with the removal efficiency increasing with the adsorbent dosage until equilibrium is reached. When CDW was used, the removal efficiency rose from 52.46 to 74.59% when the adsorbent amount rose from 0.1 to 0.7 g. However, when both acid- and base treated cow dung were used, there was a tremendous increase in the adsorption efficiency from 58.11 to 86.89% and from 55.27 to 80.38% respectively on adjusting the adsorbent amount from 0.1 to 0.5 g. It was noticed that for the raw cow dung, maximum adsorption was attained at adsorbent amount of 0.7 g, whereas, for both the acid- and base treated samples, maximum adsorption was attained at 0.5 g. This implies that aside the fact that the treated samples performed better than the raw samples, smaller amount of the treated samples are needed to reach equilibrium. The rise in adsorbed amount could be ascribed to increase in the number of available sites of adsorption sites thereby increasing the removal efficiency[2,3]. More active sites are provided for uptake of the pollutant with surge in the quantity of the adsorbent in solution, but a point is reached when saturation of these active sites occurs and as such, the removal rate declined as observed in this study when the adsorbent amount was above 0.5 g for treated sample and 0.7 g for the raw adsorbent[2,3]. The work done by Akram et al.[37] found that

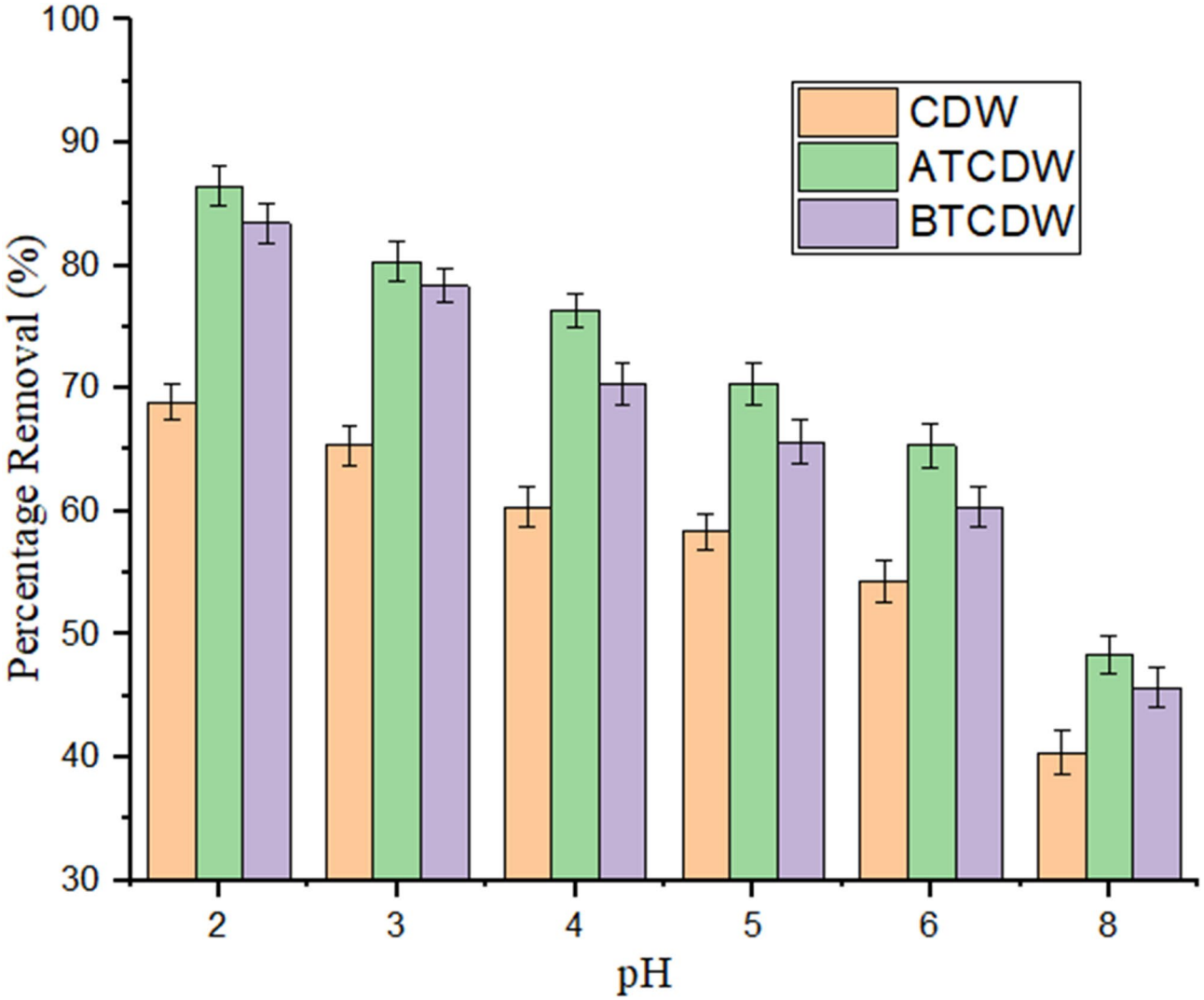

Fig. 6. Role of pH on the uptake process of ARS by CDW, ATCDW and BTCDW.

when the dosage of biosorbent was increased, it resulted in a higher percentage of ARS removal and optimum quantity of biosorbent of 0.9 g was sufficient to achieved maximum adsorption a maximum removal percentage of 82.264%. This was attributed to available large surface area containing the receptor groups of the adsorbent.

Effects time of contact and initial pollutant concentrations

Figure 8 illustrates the role of shaking time and pollutant concentration on the uptake performance of the adsorbents. The capacity adsororption of the three tested adsorbents for Alizarin Red S (ARS) shows a significant surge at the beginning of the reaction, and then reduced as the reaction progresses, ultimately reaching an equilibrium state. The capacities of adsorption for CDW and ATCDW rose from 5.38 to 18.15 mg/g (Fig. 8a) and from 9.14 to 24.52 mg/g (Fig. 8c) by extending the contact time from 20 to 100 min at ARS concentration of 50 mg/L. In contrast, the capacity of BTCDW rose from 7.85 to 21.18 mg/g (Fig. 8b) as the shaking time was extended from 20 to 80 min at the same 50 mg/L of ARS. At a higher ARS value of 300 mg/L, the amount of ARS adsorbed by CDW and ATCDW increased from 19.58 to 56.82 mg/g and from 23.57 to 88.43 mg/g, when the contact time was adjusted from 20 to 100 min. Meanwhile, the sorption potency of BTCDW surged from 22.44 to 75.46 mg/g when the equilibrium time was extended from 20 to 80 min at 300 mg/L ARS concentration. The initial rise in adsorption capacity at the start of the reaction is ascribed to the availability of vacant receptors on the adsorbent's surface, which facilitates the diffusion of ARS molecules. But when the reaction continues, the empty receptors were filled up, leading to a decrease in the reaction rate and a subsequent reduction in the adsorbent performance towards ARS uptake.

Nawaz et al.[9] observed that the trend of adsorption percentage of ARS increases with the shaking time, reaching its maximum at 45 min for magnetic *Dalbergia sissoo* and 60 min for *Dalbergia sissoo* and thereafter declines. They opined further that at the start, the sorption rate was rapid as the dye molecules quickly adhered to the outer surface of the adsorbent, owing to the availability of vacant binding sites. Similarly, data by Akram et al.[37] exhibited that the adsorption of ARS by adsorbent rose with greatly with an increase in contact time up to a

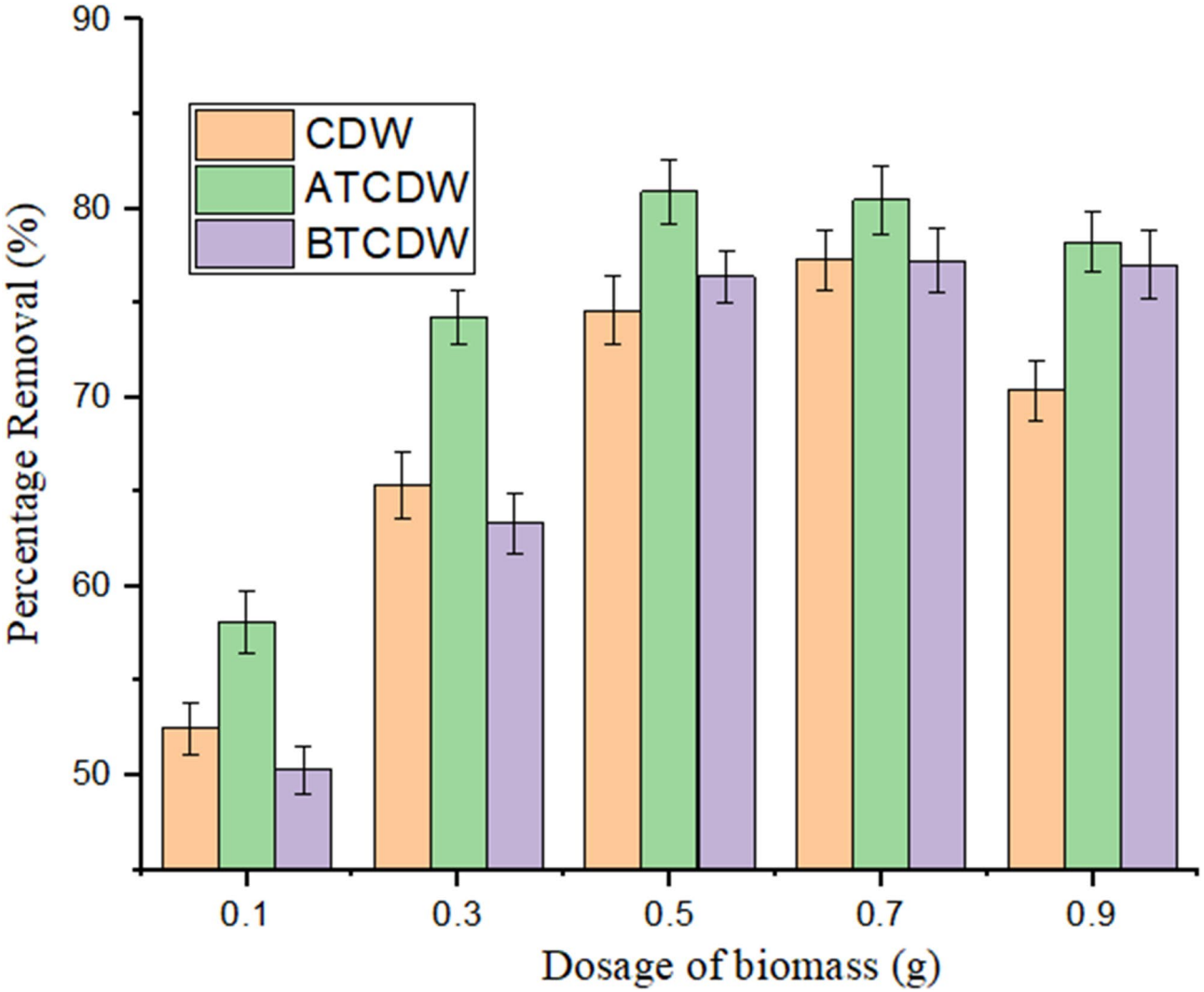

Fig. 7. The role of biomass amount on the uptake of ARS by CDW, ATCDW and BTCDW.

stage, and thereafter became almost constant with equilibrium achieved after 30 min. Imamea et al.[38] observed that the amount of dye adsorbed by biomass rose over time and attaining equilibrium at 50 min of contact time and this was because the adsorbent's surface initially has active sites available for use. After this time (the equilibrium time), there is a decrease in adsorption efficiency because fewer free sites remain on the adsorbent's surface.

In the study on the effect of pollutant concentration, it was noticed that as the ARS concentration rose, the capacity of adsorption equally rose up (Fig. 7). The capacity of adsorption CDW, ATCDW and BTCDW surged with the concentration of the pollutant. The rise in the capacity of adsorption by the adsorbents with increase in pollutant concentration is essential driving force to break way from the mass transfer resistance. With this driving force, more molecules of the pollutant are transported from the solution to the surface of the adsorbents, leading to higher ARS removal[37–39]. In the study conducted by Nawaz et al.[9] on the influence of the initial ARS concentration on the removal percentage ARS by *Dalbergia sissoo* and magnetic *Dalbergia sissoo* show that the removal efficiency of ARS rose with an increases in the initial ARS concentration and an optimal value of 66.7% for DS and 97.89% for DSMNC when the other parameters are fixed.This increase in the ARS amount is due to an enhances the driving force for mass transfer, causing an increases in the amount of adsorbed ARS.

Kinetics studies

The kinetics models of pseudo-first-order (PFO), pseudo-second-order (PSO), and intraparticle diffusion kinetics were used to fit the experimental data. The constants from these models were computed their linear forms as indicated in Fig. 9 and represented in Table 1. The adsorbed ARS amount at time t (mg g^{-1}) and the equilibrium adsorption capacity (mg g^{-1}) are given as Q_t and Q_e; where the rate constants from the PFO (min^{-1}) and PSO (g mg/min^{-1}) models are given as k_1 and k_2, while t denotes time (min). Where C_i is the intercept from the intraparticle diffusion model. The kinetics variables values obtained are as listed in Table 2. The results obtained using the CDW and ATCDW show that the correlation coefficients (R^2) from the PSO model were

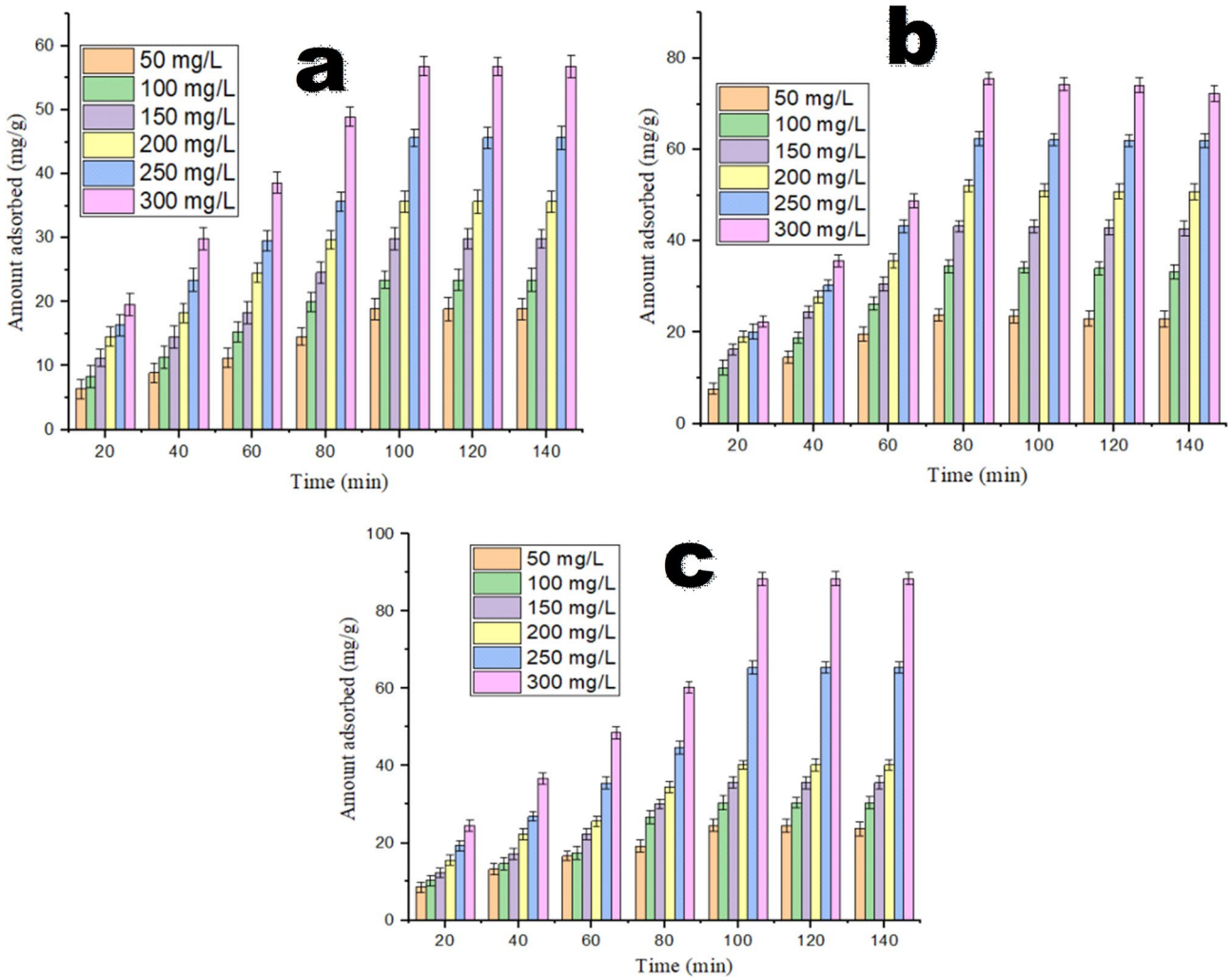

Fig. 8. The role of shaking time and ARS concentration on the uptake process of ARS by (**a**) CDW, (**b**) BTCDW and (**c**) ATCDW.

greater when compared with those from the PFO kinetic model; besides, the calculated the Q_e values of the PSO model were closer to those of experimental data. Furthermore, from the smaller values of the sum of error squares (SSE, %) computed for PSO, it can be said that the adsorption of ARS by CDW and ATCDW are governed by the PSO model and the adsorption process is controlled by chemical process[2,3]. The PFO model fits the data from the base treated cow dung waste on the strength of the higher values obtained from the correlation coefficients (R^2) and the closeness of the computed Q_e values with experimental data. This was corroborated from the smaller values of the sum of error squares (SSE, %), thus, suggesting that the rates of adsorption of ARS by BTCDW is controlled by physical process[40,41].

This observation was equally supported by the similarity observed between the computed and experimental Q_e values the adsorption process and this imply that uptake of ARS by ATCDW is chemical process[42–44]. The intraparticle diffusion model plots are given in Fig. 9c which depict three regions of adsorption beginning with a sharp stage which is due to external instantaneous adsorption. The stage two is attributable to intraparticle diffusion which involves a gradual adsorption process, and the final step is the equilibrium stage involving the uptake of the dye molecules which is controlled by physical process[2,40,42–44]. It was observed that none of plots when through the origin, and this suggests that the rate-controlling step is not only governed by intraparticle diffusion model, and as such, the rate limiting process involves some other mechanisms[2].

Adsorption isotherm

To further investigate the mechanism of Alizarin Red S adsorption by the various prepared adsorbents, mathematical models of pseudo-first order, pseudo-second order, and intra-particle diffusion kinetics and equilibrium isotherms of Langmuir, Temkin, Freundlich, and Dubinin-Radushkevich were employed using linear regression tool as listed in Table 1. where the ARS adsorbed amount at equilibrium (mg g^{-1}) and the adsorption maximum capacity (mg g^{-1}) are denoted as q_e and q_m respectively, the concentration at equilibrium (mg·L^{-1}) is given as C_e, the affinity between adsorbent and solute which defines Langmuir constants in L mg^{-1} is represented as R_L[3]:

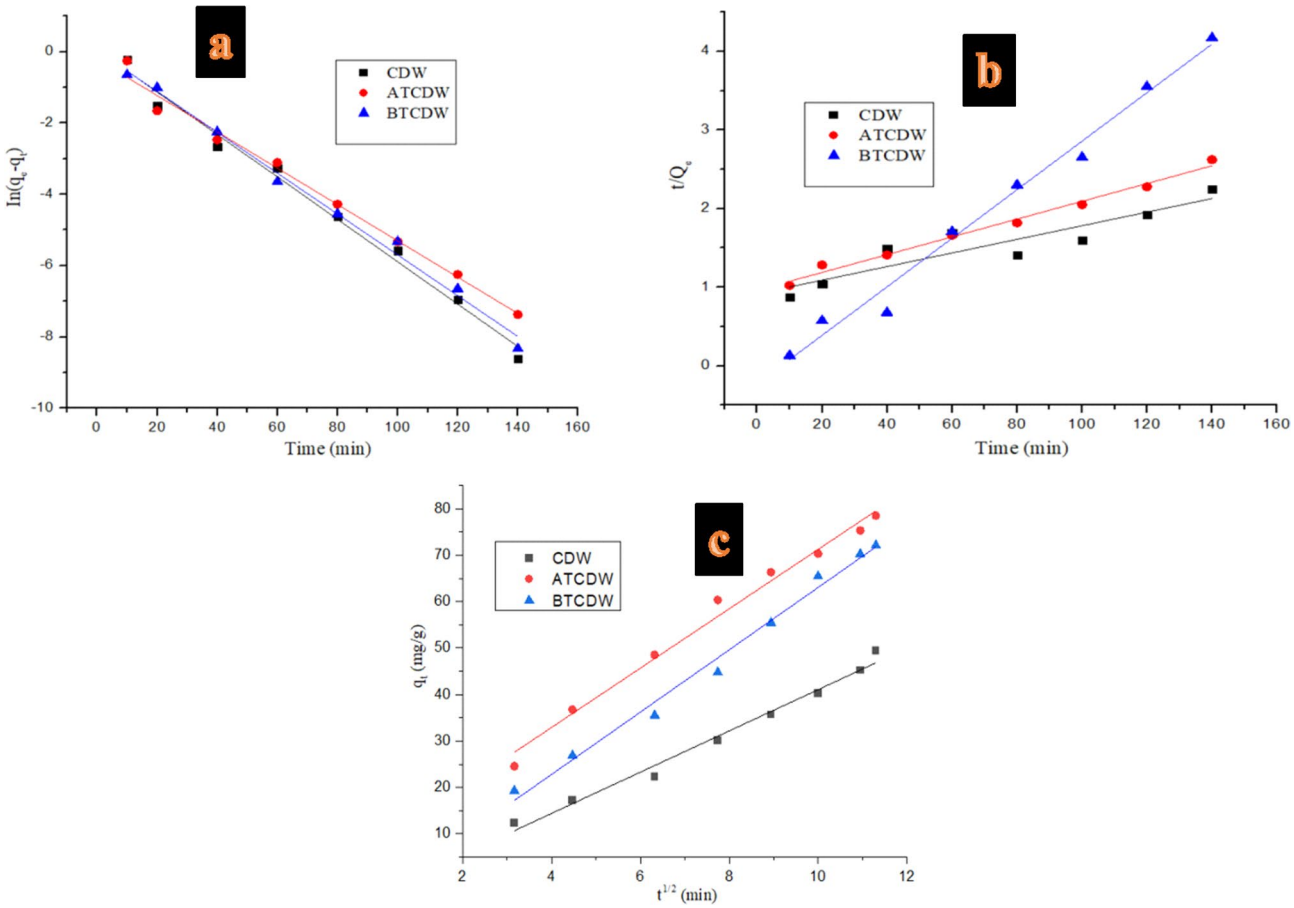

Fig. 9. Kinetics of (**a**) PSF, (**b**) PSO and (**c**) intraparticle diffusion models for the uptake of ARS by CDW, BTCDW and ATCDW.

Kinetics model	Linear form	References
PFO	$In\,(Q_e - Q_t) = InQ_e - k_1 t$ (3)	Qurrat-ul et al.[5]. Ogundiran et al.[2]. Ofudje et al.[4] Foroutan et al.[45] Peighambardoust et al.[46],
PSO	$t/Q_t = 1/(k_2 Q_e) + t/Q_t$ (4)	
Intra-particle diffusion	$Q_t = k_{id} t^{1/2} + C_i$ (5)	
Langmuir	$C_e/Q_e = 1/(Q_{max} K_L) + (1/Q_{max})\, C_e$ (6)	Kausar et al.[42], Zhou et al.[43], Hamzeh et al.[44], Peighambardoust et al.[46], Chengyu et al.[47], Foroutan et al.[48]
Freundlich	$Inq_e = InK_f + \frac{1}{n} C_e$ (7)	
Temkin	$Q_e = (RT/b)\, lnK_T + (RT/b)\, lnC_e$ (8)	
D-R	$InQ_e = InQ_m - InK_{DR}^{\varepsilon 2}$ (9)	
Polanyi potential of D-R	$\in = RTIn(1 + \frac{1}{C_e})$ (10)	
Mean adsorption energy of D-R	$E = \frac{1}{\sqrt{2K_{DR}}}$ (11)	

Table 1. Kinetics models and equilibrium adsorption isotherms including their linear forms.

$$R_L = \frac{1}{1 + bC_o}$$

where the constant of Langmuir and initial ARS concentration are given as b and Co. The values of R_L can be utilized to elucidate the type of the isotherm such as irreversible when $R_L = 0$, but when $0 < R_L < 1$, it's said to be favorable, whereas it's linear should $R_L = 1$ and becomes unfavorable when $R_L > 1$[3]. The sorption capacity of the Freundlich constants (mg g^{-1}) (L mg^{-1}) $^{1/n}$ is denoted as K_F the sorption intensity of the Freundlich

CDW												
		First order				Second order				Intra particle diffusion		
Ce	$Qe_{(exp)}$	$Qe_{(cal)}$	k_1	R^2	% SSE	$Qe_{(cal)}$	k_2	R^2	% SSE	K_p	C_i	R^2
25.670	20.221	15.470	0.225	0.912	0.312	19.312	0.181	0.964	0.038	0.103	0.113	0.953
30.880	29.160	23.222	0.264	0.825	0.425	13.425	0.201	0.987	0.016	0.156	0.126	0.952
45.722	42.310	30.183	0.288	0.711	0.511	42.511	0.245	0.986	0.025	1.73	0.242	0.966
56.284	51.260	35.360	0.476	0.902	0.602	49.602	0.337	0.983	0.012	1.203	0.504	0.975
77.282	56.820	45.220	0.527	0.848	0.348	56.348	0.386	0.986	0.014	2.423	0.833	0.967
85.101	67.203	56.103	0.326	0.921	0.021	67.021	0.231	0.978	0.012	2.681	1.250	0.947
ATCDW												
24.57	24.524	23.421	0.262	0.848	0.104	19.241	0.162	0.988	0.004	0.243	0.245	0.789
40.33	33.424	32.040	0.351	0.716	0.015	27.573	0.263	0.976	0.005	0.563	0.543	0.889
54.27	35.660	36.253	0.464	0.915	0.019	40.623	0.351	0.985	0.009	0.783	1.235.	0.928
67.34	40.230	41.371	0.711	0.934	0.055	53.281	0.675	0.994	0.005	1.145	1.425	0.939
75.62	65.450	64.270	0.765	0.794	0.028	59.825	0.751	0.979	0.008	1.225	3.226	0.945
91.14	72.484	73.102	0.125	0.828	0.044	65.102	0.321	0.989	0.004	3.307	5.173	0.869
BTCDW												
20.331	23.780	22.31	0.062	0.985	0.009	23.780	19.212	0.115	0.877	0.672	2.618	0.894
38.654	34.450	33.26	0.027	0.967	0.007	34.450	29.340	0.135	0.924	1.213	3.449	0.938
55.170	43.210	42.35	0.331	0.983	0.006	43.210	40.220	0.183	0.892	1.530	5.291	0.946
64.420	52.170	51.22	0.338	0.993	0.005	52.170	49.791	0.225	0.912	2.245	5.361	0.974
84.722	62.350	64.98	0.447	0.967	0.007	62.350	54.652	0.271	0.943	5.0034	8.313	0.984
93.331	73.78	75.31	0.062	0.985	0.019	73.78	68.120	0.115	0.877	6/201	8.360	0.922

Table 2. Kinetics variables of ARS uptake by CDW, ATCDW and BTCDW.

constants is given as n, the adsorption concentration (mg L^{-1}). From the D-R, the amount of pollutant adsorbed per weight unit of adsorbent after equilibrium (mol/g) is given as Q_e, while q_m denote adsorption maximum capacity (mol/g) of monolayer coverage, the mean sorption energy associated with activity coefficient mol^2/kJ^2 is depicted as K_{DR}, the Polanyi potential constant is given as ε, R (8.3145 J mol^{-1} K^{-1}) is ideal gas constant, and T stands for absolute temperature in K. Figures 10 and 11 show the isotherms plots, while Tables 1 and 3 presents the isotherms equations, their constants and the respective values obtained. On the basis of the coefficient correlation (R^2), the CDW and ATCDW obey the Freundlich isotherm indicating a heterogenous adsorption process, whereas, the adsorption ARS by BTCDW follows Langmuir isotherm which implies monolayer adsorption and the adsorption performance of adsorbent surface is uniform[42,43]. The monolayer maximum capacities from the Langmuir isotherm for CDW, ATCDW and BTCDW are computed to be 58.241, 87.543 and 61.370 mg/g, respectively, with the ATCDW significantly higher than the remaining two adsorbents. The computed values of R_L for the three adsorbents were found to be 0.720, 0.322 and 0.171 for CDW, ATCDW and BTCDW suggesting a favorable character toward ARS adsorption. The value of E is very important in predicting whether the adsorption occurred via physical or chemical process[43,47,48]. The adsorption of ARS by CDW and ATCDW can be chemical in nature since the calculated value of E is bigger than 8 kJ/mol but the adsorption by BTCDW is physical because the value of E computed is less than 8 kJ/mol[43,44]. Table 4 gives the different adsorption capacities of adsorbents in literature in comparison with those CDW, ATCDW and BTCDW adsorbents for the eradication of ARS. As can be seen, these three adsorbents compete favorably with others in literature which is a confirmation of their applicability in the ARS removal from contaminated water.

Temperature effect and thermodynamics study

Temperature is very crucial factor for the uptake of pollutant by adsorbent and to evaluate if the adsorption of ARS is exothermic or endothermic, studies were done at varied temperatures (25–65 °C) as shown in Fig. 12a. The elimination of ARS surge with a rise in temperature, which suggests the nature of the process to be endothermic. When the adsorption process temperature was raised from 25 to 45 °C, the percentage adsorption of CDW, ATCDW and BTCDW increased from 52.36 to 70.33%, 51.68 to 74.65% and from 51.26 to 72.33% respectively. Maximum adsorption of ARS was attained at a temperature of 45 °C and above this temperature, the adsorption appeared to be uniform and as such, and for subsequent reactions, a temperature of 45 °C was chosen. When the temperature increases, solvent (water) and solid surface interaction reduces which expose larger proportions of the adsorption sites for the uptake of the dye molecules[36,41]. With this, the interaction between adsorbents and dye molecules increases. However, at a much higher temperature, the possibility of bond rapture, could be responsible for the declined in the sorption ability of the adsorbent[36]. Thermodynamics parameters of enthalpy change (ΔH), entropy change (ΔS), and free energy change (ΔG) were determined using Eq. 12 to 14 below[5,40]:

$$\Delta G^o = -RT \ln K_D \tag{12}$$

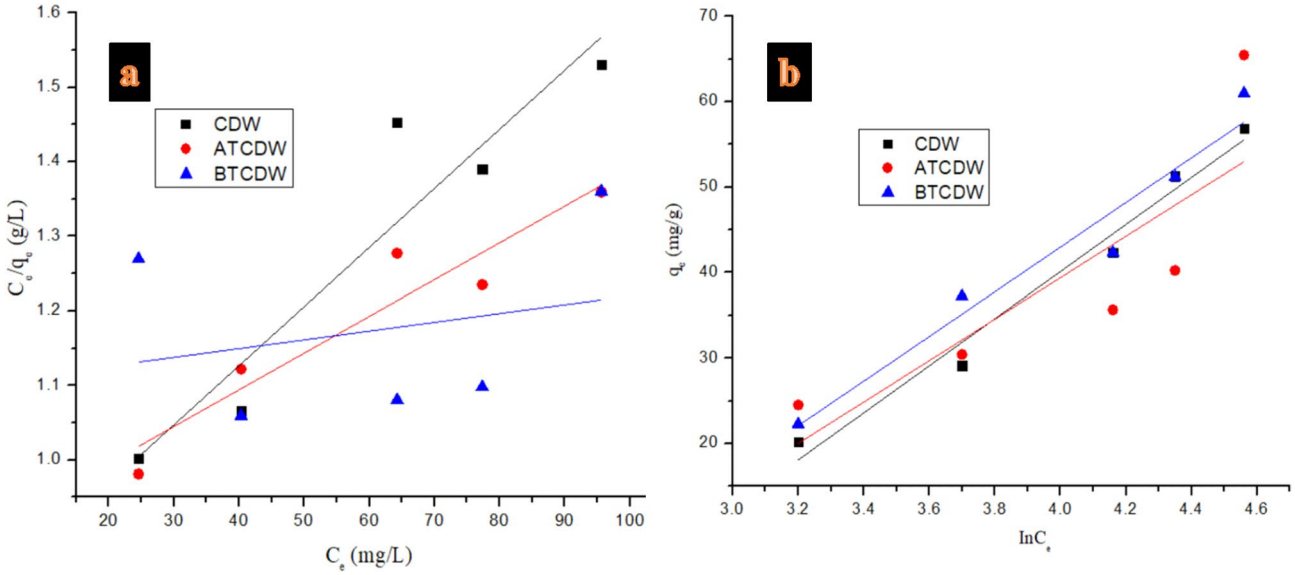

Fig. 10. Isotherms of (**a**) Langmuir, and (**b**) Temkin in the adsorption of ARS by CDW, ATCDW, and BTCDW.

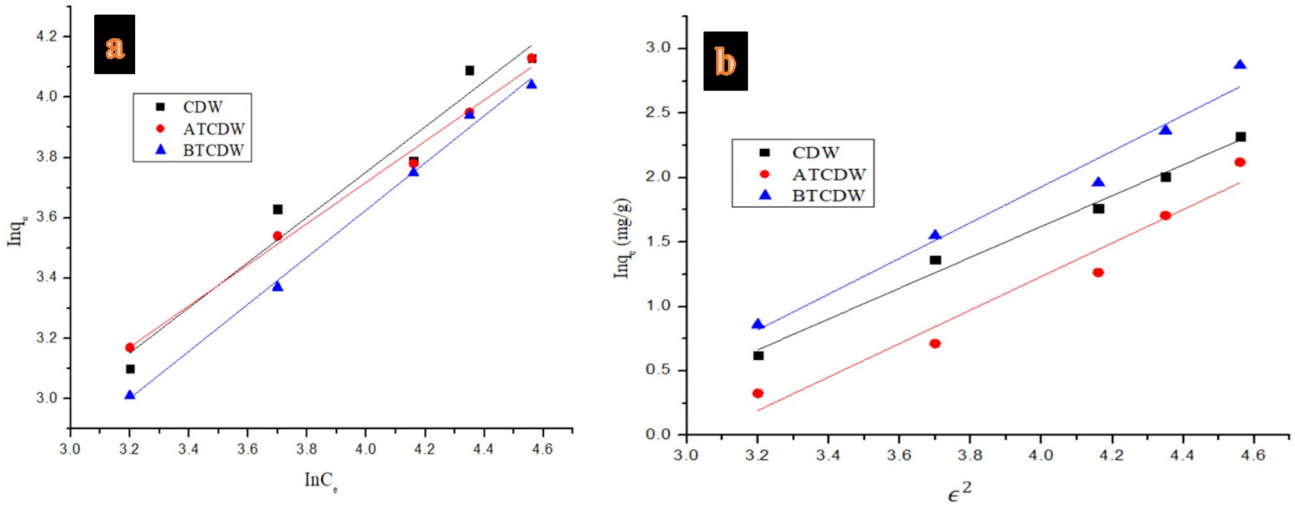

Fig. 11. Isotherms of (**a**) Freundlich, and (**b**) D–R in the adsorption of ARS by CDW, ATCDW, and BTCDW.

$$\Delta G^o = \Delta H^o - T\Delta S \tag{13}$$

$$Ink_D = \frac{\Delta S}{R} - \frac{\Delta H}{R} \times \frac{1}{T} \tag{14}$$

where K_D denote the equilibrium constant which was obtained from the graph of (qe/Ce) against qe, R which is valued at 8.314 J K^{-1} mol^{-1} denote the universal gas constant, and T represents temperature in Kelvin. The values of ΔH and ΔS were determined the slope and intercept from the plot of ln K_o against the inverse of the temperature (1/T), as illustrated in Fig. 12b. As revealed in Table 5, the ΔH values indicate that the elimination process of ARS by CDW and ATCDW could be considered as endothermic and chemical adsorption in nature (ΔH is greater than 40 kJ mol^{-1}), whereas that of BTCDW physical in nature (ΔH is less than 20 kJ mol^{-1})[8,48]. In a similar way, judging on negative values of ΔG, the elimination process of ARS by the three adsorbents is spontaneous and feasible with better preference of ARS particles for the adsorbents. The negative values of ΔG were observed to increase with rising temperature, further confirming the endothermic nature of sorption process. The entropy changes values obtained for CDW, ATCDW and BTCDW are 3.71, 1.35 and 2.46 kJ mol^{-1} K^{-1} respectively and since the values are positive, it inferred an increase in randomness of the uptake process and reflects the affinity of the adsorbents for the ARS molecules at elevated temperature[5,41].

Models	Parameters	CDW	ATCDW	BTCDW
Langmuir	q_L (mg/g)	58.241	87.543	61.37
	R_L	0.72	0.322	0.171
	R^2	0.958	0.949	0.998
Freundlich	K_F ((mol g^{-1}) (mol L^{-1})$^{-1/n}$	36.822	68.421	40.816
	1/n	0.470	0.140	0.172
	R^2	0.997	0.996	0.924
Temkin	A (L/g)	0.958	0.346	0.867
	B (mg/g)	40.021	66.301	60.410
	R^2	0.981	0.936	0.954
Dubinin–Radushkevich (D–R)	q_m (mg/g)	50.221	88.011	65.024
	E (kJ/mol)	10.265	12.114	6.233
	β (mol kJ^{-1})^2	0.422	0.152	0.352
	R^2	0.976	0.957	0.946

Table 3. Isotherms parameter for the adsorption ARS by CDW, ATCDW and BTCDW adsorbents at 45 °C.

Adsorbent	Adsorption capacity (mg/g)	References
Alhagi maurorum	8.203	Akram et al.[37]
Weed *Mikania micrantha*	46.51	Gautam et al.[49]
Lantana camara	1.16	Gautam et al.[50]
Iron-based Fe-BTC MOF	80	Giulia et al.[51]
Polypyrrole-coated magnetic nanoparticles	116.3	Gholivand et al.[52]
Magnetic chitosan	40.1	Fan et al.[53]
Olive stone	16.01	Albadarin et al.[54]
Multiwalled carbon nanotubes	135.2	Fernando et al.[5]
Biomassbased activated carbon	91.695	Bhomick et al.[11]
Multiwalled carbon nanotubes	161.290	Ghaedi et al.[40]
Activated clay modified by iron oxide	32.7	Feng et al.[41]
CDW	58.241	This present study
ATCDW	87.543	This present study
BTCDW	61.37	This present study

Table 4. Comparison of adsorption capacities in literature with CDW, ATCDW and BTCDW.

Mechanism of adsorption

The relationship between the ARS molecules and the adsorbent can be further understood through adsorption mechanism. As seen from the infrared spectra of adsorbents, the surface of the adsorbent was composed of functional groups like O–H, C=O, and C–O which when submerged in a solution with pH less than 4.0, they become protonated, and the CDW surface acquires a positive charge. On the hand, the ARS molecules are negatively charged due to its' anionic nature. Thus, an electrostatic bond is formed between the ARS particles which are negatively charged and the positively charged CDW functional groups that have been protonated and as such, the mechanism of ARS dye uptake by the cow dung waste could be an electrostatic interaction. This view was supported in literature by the study conducted by Fernando et al.[5]. where it was stated that the uptake of anionic dye (ARS) by carbon nanotubes at pH 2 occurred via electrostatic attraction of the positively charged carbon nanotube and the negatively charged anionic molecules of ARS. Judging from thermodynamic study as based on the values of ΔH, the mechanism of ARS adsorption by CDW and ATCDW proceed through chemical adsorption since ΔH is between 80 and 450 kJ mol^{-1}, whereas the mechanisms of BTCDW is physical in nature with ΔH value less than 20 kJ mol^{-1}[5,23,40,48].

Desorption overview

The desorption data for CDW, BTCDW, and ACTCDW are revealed in Fig. 13. For raw cow dung, desorption decreases steadily from 76.7 to 52.3% as the number of desorption study declines from cycle one to six, suggesting that raw dung's ability to release adsorbed substances declines gradually, though this trend was little within the first three cycles. This suggests that untreated cow dung is less effective at retaining adsorbed compounds, potentially due to a less-developed surface structure or chemical interactions that might otherwise enhance retention. For the base-treated cow dung sample on the other hand, similar trend was seen, but the desorption values are higher, decreasing from 82.3% at first cycle to 68.9% at sixth cycles. This indicates that base treatment modifies the surface of the cow dung material such that it improves its ability to retain adsorbed ARS molecules when compared to the raw sample. In the case of the acid-treated cow dung, it consistently shows the highest

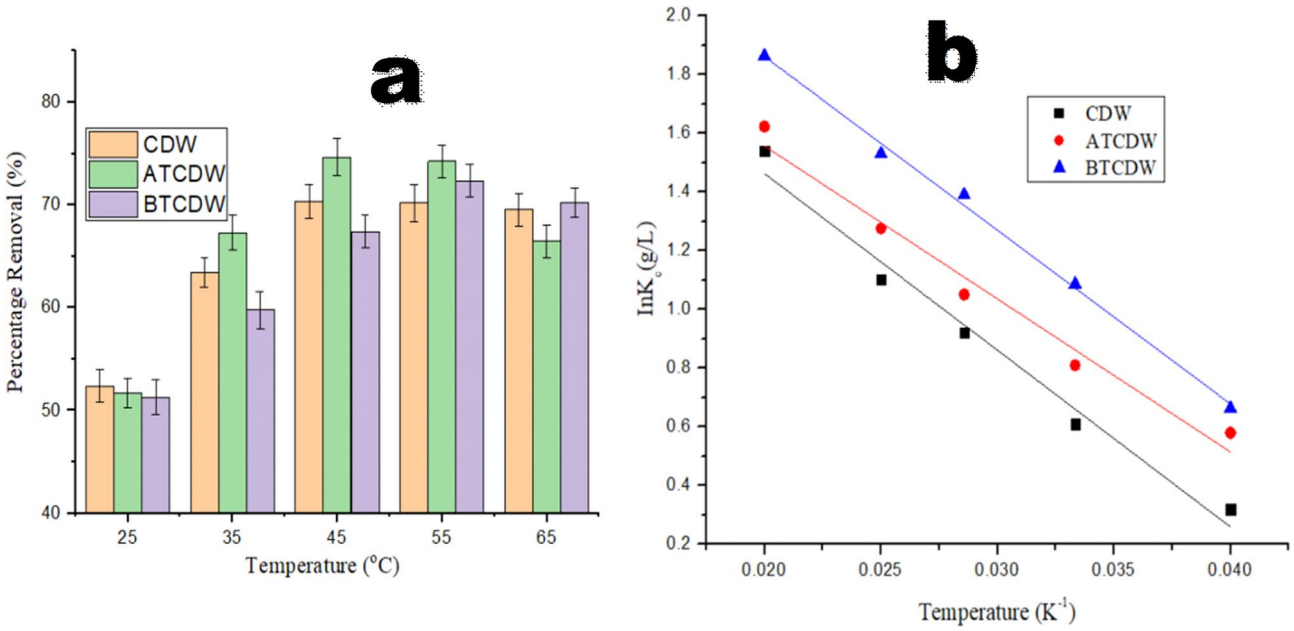

Fig. 12. Plots of (**a**) temperature effect and (**b**) thermodynamics study in the adsorption of ARS by CDW, ATCDW, and BTCDW.

	CDW			ATCDW			BTCDW		
T (K)	ΔG (kJ/mol)	ΔH (kJ/mol)	ΔS (kJ/mol/K)	ΔG (kJ/mol)	ΔH (kJ/mol)	ΔS (kJ/mol/K)	ΔG (kJ/mol)	ΔH (kJ/mol)	ΔS (kJ/mol/K)
298	− 1.89	48.124	3.710		95.220	1.350		7.550	2.460
303	− 2.65			− 1.25			− 1.33		
308	− 4.22			− 2.33			− 2.21		
318	− 6.26			− 4.46			− 3.67		
328	− 7.22			− 5.56			− 3.93		
338	− 7.74			− 6.25			− 5.66		

Table 5. Thermodynamics values for the adsorption of ARS by CDW, ATCDW and BTCDW.

desorption values, ranging from 85.4% at first cycle to 70.2% at sixth cycles. This could be as a result of the acid treatment which altered the surface charge of the dung, and enhanced its ability to retain adsorbed ARS molecules. Comparing the three materials, the acid treatment appears to have more retention ability towards the adsorbed molecules of ARS, with consistently higher desorption values across all measurements. This could be due to the increased surface area, altered surface chemistry, and possibly the breakdown of organic matter.

Potential contamination from untreated cow dung waste (CDW) and future considerations

One important consideration in this study is the potential risk of contamination when using untreated cow dung waste (CDW) in environmental processes. Untreated CDW may contribute to pollution, introducing bacteria, heavy metals, and other pollutants that are not digested by cows, such as microplastics and other chemical residues. In our experimental setup, we have made efforts to minimize the risk of contamination. Prior to any treatments, the cow dung was thoroughly washed to remove any easily removable external contaminants and sun dried. The growth of microbs was also hindered by adopting acidic pH range. However, we recognize that further analysis of potential microbial presence, as well as the identification of heavy metals and microplastic contamination, would strengthen the environmental safety aspects of the study. Thus, a more thorough assessment of the impact of untreated CDW on distilled water could be a future studies to ensure a complete evaluation of the material's environmental impact.

Conclusions

This study examined the use of cow dung waste (CDW), acid-treated cow dung waste (ATCDW), and base-treated cow dung waste (BTCDW) as low-cost adsorbents for the uptake of Alizarin Red S dye. The influence of various factors, like temperature, shaking time, ARS concentration, pH, and adsorbent amount, on the sorption efficiency was studied. The optimal adsorption conditions were found to be at a pH of 2.0 and a temperature of 45 °C, with contact times of 80 min for BTCDW and 100 min for both CDW and ATCDW. Kinetic studies showed that the adsorption of ARS by CDW and ATCDW followed the pseudo-second-order model, whereas

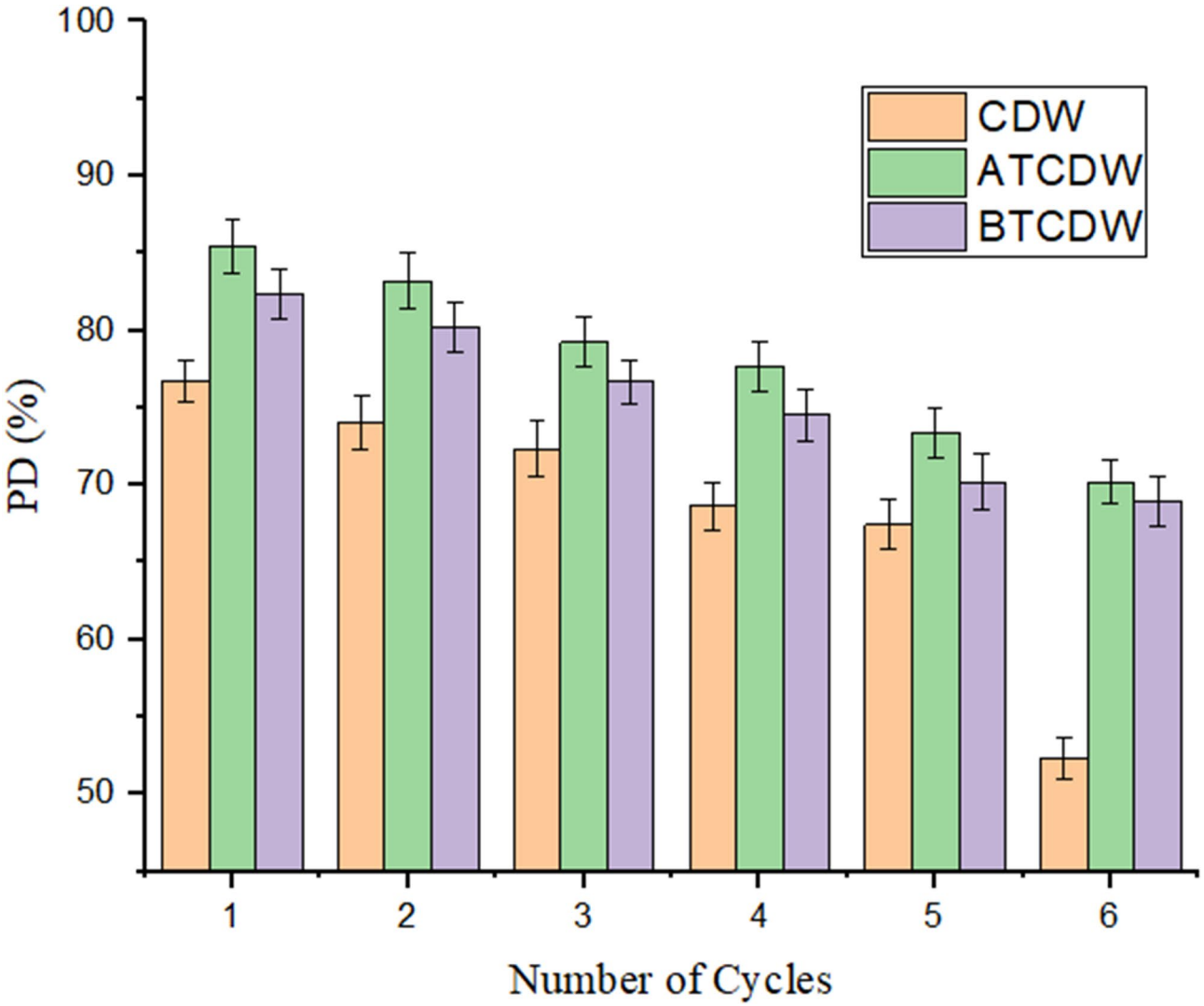

Fig. 13. Desorption studies.

BTCDW adhered to the pseudo-first-order model. Thermodynamic examination revealed that the adsorption process was physical for CDW and chemical for both ATCDW and BTCDW, as reflected in their enthalpy values. The treated adsorbents exhibited superior performance compared to the raw material, highlighting the enhanced sorption capacity following treatment. Desorption data reveals that acid and base treatment enhanced the dung's ability to retain adsorbed ARS molecules. Overall, the findings demonstrate that cow dung waste, particularly when treated with acid, can be effectively utilized as cost-efficient material and sustainable for the elimination of organic contaminants like Alizarin Red S from wastewater.

Data availability

The datasets used and/or analysed during the current study available from the corresponding author on reasonable request.

Received: 4 April 2025; Accepted: 4 August 2025
Published online: 13 August 2025

References

1. Kingsley, O. I. et al. Removal of pollutants from aqueous media using cow dung-based adsorbents. *Curr. Res. Green. Sustain. Chem.* **5**, 100300. https://doi.org/10.1016/j.crgsc.2022.100300 (2022).
2. Ogundiran, A. A., Ofudje, E. A., Ogundiran, O. O. & Adewusi, A. M. Cationic dye adsorptions by eggshell waste: kinetics, isotherms and thermodynamics studies. *Desalin. Water Treatment.* **280** (2022) 157–167. https://doi.org/10.5004/dwt.2022.29080 (2022).
3. Uzosike, A. O. et al. Magnetic supported activated carbon obtained from walnut shells for Bisphenol–A uptake from aqueous solution. *Appl. Water Sci.* **12**, 201. https://doi.org/10.1007/s13201-022-01724-1 (2022).

4. Ofudje, E. A. et al. Eggshell derived calcium oxide nanoparticles for Toluidine blue removal. *Desalin. Water Treatment*. **247**, 294–308. https://doi.org/10.5004/dwt.2022.28079 (2022).
5. Fernando, M. M. et al. Adsorption of Alizarin Red S Dye by carbon nanotubes: An experimental and theoretical investigation. *J. Phys. Chem. C*. **120**, 18296–18306. https://doi.org/10.1021/acs.jpcc.6b03884 (2016).
6. Ghaedi, M., Hassanzadeh, A. & Kokhdan, S. N. Multiwalled carbon nanotubes as adsorbents for the kinetic and equilibrium study of the removal of Alizarin red S and Morin. *J. Chem. Eng. Data*. **56**, 2511–2520 (2011).
7. Fu, F., Gao, Z., Gao, L. & Li, D. Efective adsorption of anionic dye, Alizarin red S, from aqueous solutions on activated clay modifed by iron oxide. *Ind. Eng. Chem. Res.* **50**, 9712–9717. https://doi.org/10.1021/ie200524b (2011).
8. Moorthy, A. K., Shukla, S. P., Govindarajan, R. B., Kumar, K. & Bharti, V. S. Application of microalgal physiological response as biomarker for evaluating the toxicity of the textile dye Alizarin red S. *Bull. Environ. Contam. Toxicol.* **109**, 401–408. https://doi.org/10.1007/s00128-022-03525-3 (2022).
9. Nawaz, S. et al. Kinetics and thermodynamics investigations of efficient and eco-friendly removal of Alizarin red S from water via acid-activated dalbergia Sissoo leaf powder and its magnetic iron oxide nanocomposite. *Front. Chem.* **12**, 1457265. https://doi.org/10.3389/fchem.2024.1457265 (2024).
10. Hassan, A., Victor, K., Karim, H. & Mona, K. A review of environmental impact of Azo dyes. *Int. J. Res. Rev.* **10**(6). https://doi.org/10.52403/ijrr.20230682 (2023).
11. Bhomick, P. C. et al. Alizarin red S adsorption onto biomassbased activated carbon: optimization of adsorption process parameters using Taguchi experimental design. *Int. J. Environ. Sci. Technol.* https://doi.org/10.1007/s13762-019-02389-1 (2019).
12. Qurrat-ul, A. et al. Anionic Azo dyes removal from water using amine-functionalized cobalt–iron oxide nanoparticles: a comparative time-dependent study and structural optimization towards the removal mechanism. *RSC Adv.* **10**, 102. https://doi.org/10.1039/c9ra07686g (2020).
13. Selvaraj, V., Karthika, T. S., Mansiya, C. & Alagar, M. An over review on recently developed techniques, mechanisms and intermediate involved in the advanced Azo dye degradation for industrial applications. *J. Mol. Struct.* **1224**, 129195 (2021).
14. Esmaeili, H., Foroutan, R., Jafari, D. & Rezaei, M. A. Effect of interfering ions on phosphate removal from aqueous media using magnesium oxide@ferric molybdate nanocomposite. *Korean J. Chem. Eng.* **37**, 804–814. https://doi.org/10.1007/s11814-020-0493-6 (2020).
15. Massrour, A., Peighambardoust, S. J., Foroughi, M., Foroutan, R. & Ramavandi, B. Crystal Violet removal by sodium alginate-g-polyacrylamide/ hydroxyapatite/ Cu-Fe LDH nanocomposite. *Environ. Technol. Innov.* **38**, 104149. https://doi.org/10.1016/j.eti.2025.104149 (2025).
16. Amaterz, E. et al. Hierarchical flower-like $SrHPO_4$ electrodes for the photoelectrochemical degradation of Rhodamine B. *J. Appl. Electrochem.* **50**, 569–581. https://doi.org/10.1007/s10800-020-01416-1 (2020).
17. Abshirini, Y., Esmaeili, H. & Foroutan, R. Enhancement removal of Cr(VI) ion using magnetically modified MgO nanoparticles. *Mater. Res. Express*. **6** (12), 125513. https://doi.org/10.1088/2053-1591/ab56ea (2019).
18. Yang, C. et al. Fabrication and characterization of a high performance polyimide ultrafiltration membrane for dye removal. *J. Colloid Interface Sci.* **562**, 589–597. https://doi.org/10.1016/j.jcis.2019.11.075 (2020).
19. Dutta, S. et al. Contamination of textile dyes in aquatic environment: adverse impacts on aquatic ecosystem and human health, and its management using bioremediation. *J. Environ. Manag.* **353**, 120103. https://doi.org/10.1016/j.jenvman.2024.120103 (2024).
20. Ahmad, A., Khan, N., Giri, B. S., Chowdhary, P. & Chaturvedi, P. Removal of methylene blue dye using rice husk, cow Dung and sludge biochar: characterization, application, and kinetic studies. *Bioresour Technol.* **306**, 123202 (2020).
21. Ebrahimi, A., Arami, M., Bahrami, H. & Pajootan, E. Fish bone as a low-cost adsorbent for dye removal from wastewater: response surface methodology and classical method. *Environ. Model. Assess.* **18** (6), 661–670 (2013).
22. Wongrueng, A., Rakruam, P., Siri, A. & Siyasukh, A. Synthesis of porous pig bone Char as adsorbent for removal of DBP precursors from surface water. *Water Sci. Technol.* **79** (5), 857–865 (2019).
23. Ofudje, E. A. et al. Mechanism of Cu^{2+} and reactive yellow 145 dye adsorption onto eggshell waste as low- cost adsorbent. *Chem. Ecol.* https://doi.org/10.1080/02757540.2020.1855153 (2020).
24. Yao, Z., Yang, W., Xia, M. & Ye, Y. Crab shell: a potential high-efficiency and low-cost adsorbent for dye wastewater. *Fresenius Environ. Bull.* **26** (8), 4991–4998 (2017).
25. Yusuff, A. S., Ajayi, O. A. & Popoola, L. T. Application of Taguchi design approach to parametric optimization of adsorption of crystal Violet dye by activated carbon from poultry litter. *Sci. Afr.* **13**, e00850 (2021).
26. Li, H., Yang, S., Sun, H. & Liu, X. Production of activated carbon from cow manure for wastewater treatment. *Bioresources*. **13** (2), 3135–3143 (2018).
27. Hendarto, E., Suwarno, S. & Sudiarto, P. Influence of urea-dairy cattle Dung fertilizer combinations on growth and production of mulato grass (Brachiaria hybrid Cv mulato). *Anim. Prod.* **20** (1), 29–38 (2019).
28. Joshua, B. Boosting dairy value chain in Nigeria: Lessons from Arla Foods. (2023). https://businessday.ng/features/article/boosting-dairy-value-chain-in-nigeria-lessons-from-arla-foods/. Retrieve on: 18/08/2023.
29. Kian, L. K., Jawaid, M., Ariffin, H. & Alothman, O. Isolation and characterization of microcrystalline cellulose from roselle fibers. *Int. J. Biol. Macromol.* **103**, 931–940. https://doi.org/10.1016/j.ijbiomac.2017.05.135 (2017).
30. Ilyas, R. A., Sapuan, S. M. & Ishak, M. R. Isolation and characterization of nanocrystalline cellulose from sugar palm fibres (Arenga Pinnata). *Carbohydr. Polym.* **181**, 1038–1051. https://doi.org/10.1016/j.carbpol.2017.11.045 (2018).
31. Kataoka, L. F. M. S., Hidalgo Falla, M. D. P. & Luz, S. M. D. The influence of potassium hydroxide concentration and reaction time on the extraction cellulosic jute fibers. *J. Nat. Fibers*. **19**, 1–13. https://doi.org/10.1080/15440478.2021.1934934 (2021).
32. Leite, A. L. M. P., Zanon, C. D. & Menegalli, F. C. Isolation and characterization of cellulose nanofibers from cassava root Bagasse and peelings. *Carbohydr. Polym.* **157**, 962–970. https://doi.org/10.1016/j.carbpol.2016.10.048 (2017).
33. Siqueira, G., Bras, J. & Dufresne, A. Luffa cylindrica as a lignocellulosic source of fiber, microfibrillated cellulose, and cellulose nanocrystals. *BioResources*. **5**, 727–740 (2010).
34. Vishnu Vardhini, K. J. & Murugan, R. Effect of *Laccase* and *Xylanase* enzyme treatment on chemical and mechanical properties of banana fiber. *J. Nat. Fibers*. **14**, 217–227. https://doi.org/10.1080/15440478.2016.1193086 (2017).
35. Reddy, K. O. et al. Extraction and characterization of cellulose single fibers from native African Napier grass. *Carbohydr. Polym.* **188**, 85–91. https://doi.org/10.1016/j.carbpol.2018.01.110 (2018).
36. Jeremic, S., Filipovic, N., Peulić, A. & Marković, Z. Thermodynamical aspect of radical scavenging activity of Alizarin and Alizarin red S. Theoretical comparative study. *Comp. Theor. Chem.* **1047**, 15–21 (2014).
37. Akram, B. et al. Kinetic and thermodynamic analysis of Alizarin red S biosorption by *Alhagi maurorum*: a sustainable approach for water treatment. *BMC Biotechnol.* **24**, 85. https://doi.org/10.1186/s12896-024-00913-x (2024).
38. Imamea, S. et al. Efficient adsorption of malachite green from wastewater using agricultural biosource waste: kinetic, isothermal, thermodynamic studies and mechanisms analysis.anal. *Methods Environ. Chem. J.* **8** (1), 5–25 (2025).
39. Kali, A. et al. Efficient adsorption removal of an anionic Azo dye by lignocellulosic waste material and sludge recycling into combustible briquettes. *Colloids Interfaces*. **6**, 22. https://doi.org/10.3390/colloids6020022 (2022).
40. Ghaedi, M., Hassanzadeh, A. & Kokhdan, S. N. Multiwalled carbon nanotubes as adsorbents for the kinetic and equilibrium study of the removal of Alizarin Red S and Morin M. *J. Chem. Eng. Data* **56**, 2511–2520. https://doi.org/10.1021/je2000414 (2011).
41. Feng, F., Ziwei, G., Lingxiang, G. & Dongsheng, L. Effective adsorption of anionic dye, Alizarin red S, from aqueous solutions on activated clay modified by iron oxide. *Ind. Eng. Chem. Res.* **50**, 9712–9717. https://doi.org/10.1021/ie200524b (2011).

42. Kausar, A., Bhatti, H. N. & MacKinnon, G. Equilibrium, kinetic and thermodynamic studies on the removal of U(VI) by low cost agricultural waste. *J. Colloids Surf. B.* **111**, 124–133 (2013).
43. Zhou, Y., Lu, J., Zhou, Y. & Liu, Y. Recent advances for dyes removal using novel adsorbents: a review. *Environ. Pollut.* **252**, 352–365. https://doi.org/10.1016/j.envpol.2019.05.072 (2019).
44. Hamzeh, E., Hasan, T., Farhoush, K. & Mansour, J. Kinetics, equilibrium and isotherms of Pb^{2+} adsorption from aqueous solutions on carbon nanotubes functionalized with 3-amino-5a,10a-dihydroxybenzo[b] Indeno [2,l-d]furan-10-one. *New Carbon Mater.* **34** (6), 512–523. https://doi.org/10.1016/S1872-5805(19)60027-2 (2010).
45. Foroutan, R., Tutunchi, A., Foroughi, A. & Ramavandi, B. Defluorination of water solutions and glass industry wastewater using a magnetic pineapple hydrochar nanocomposite modified with a covalent organic framework. *J. Environ. Manag.* **377**, 124651. https://doi.org/10.1016/j.jenvman.2025.124651 (2025).
46. Peighambardoust, S., Abdollahian Aghbolagh, S., Foroutan & Peighambardoust, N. S. Decontamination of crystal Violet using nanocomposite adsorbent based on pine cone Biochar modified with $CoFe_2O_4$/Mn-Fe LDH. *Sci. Rep.* **15**, 15067. https://doi.org/10.1038/s41598-025-99549-w (2025).
47. Chengyu, D., Tianyu, M., Jianyu, W. & Yanbo, Z. Removal of heavy metals from aqueous solution using carbon-based adsorbents: A review. *J. Water Process. Eng.* **37**, 101339. https://doi.org/10.1016/j.jwpe.2020.101339 (2020).
48. Foroutan, R., Tutunchi, A., Foroughi, M. & Ramavandi, B. Efficient fluoride removal from water and industrial wastewater using magnetic chitosan/β-cyclodextrin aerogel enhanced with Biochar and MOF composites. *Sep. Purif. Technol. Part.* **2** (363), 132128. https://doi.org/10.1016/j.seppur.2025.132128 (2025).
49. Gautam, P. K., Gautam, R. K., Banerjee, S., Chattopadhyaya, M. C. & Pandey, J. D. Adsorptive removal of Alizarin red S by a novel biosorbent of an invasive weed Mikania Micrantha. *Natl. Acad. Sci. Lett.* **40**, 113–116. https://doi.org/10.1007/s40009-017-0540-y (2017).
50. Gautam, R. K., Gautam, P. K., Chattopadhyaya, M. C. & Pandey, J. D. Adsorption of Alizarin red S onto biosorbent of Lantana camara: kinetic, equilibrium modeling and thermodynamic studies. *Proc. Natl. Acad. Sci. India Sect. Phys. Sci.* **84**, 495–504 (2014).
51. Machado, F. M. et al. Adsorption of reactive blue 4 dye from water solutions by carbon: experiment and theory. *Phys. Chem. Chem. Phys.* **14**, 11139–11153 (2012).
52. Giulia, R. D., Davide, T., Luca, M., Edmond, M. & Andrea, S. Adsorption of malachite green and Alizarin red S dyes using Fe-BTC metal organic framework as adsorbent. *Int. J. Mol. Sci.* **22**, 788. https://doi.org/10.3390/ijms22020788 (2021).
53. Gholivand, M. B., Yamini, Y., Dayeni, M., Seidi, S. & Tahmasebi, E. Adsorptive removal of Alizarin red-S and Alizarin yellow GG from aqueous solutions using polypyrrole-coated magnetic nanoparticles. *J. Environ. Chem. Eng.* **3**, 529–540 (2015).
54. Fan, L. et al. Removal of Alizarin red from water environment using magnetic Chitosan with Alizarin red as imprinted molecules. *Colloids Surf. B.* **91**, 250–257 (2012).
55. Albadarin, A. B. & Mangwand, C. Mechanisms of Alizarin red S and methylene blue biosorption onto Olive stone by-product: isotherm study in single and binary systems. *J. Environ. Manag.* **164**, 86–93 (2015).

Acknowledgements

The authors express their gratitude to the Deanship of Scientific Research at Northern Border University, Arar, KSA, for funding this research work through project number "NBU-FFR-2025-2985-07". Furthermore, authors wish to appreciate the financial support via Princess Nourah bint Abdulrahman University Researchers Supporting Project number (PNURSP2025R65), Princess Nourah bint Abdulrahman University, Riyadh, Saudi Arabia.

Author contributions

A.E.-R. contributed finance, A.M.B. performed the experiments, and wrote the first draft, M.S.F. performed statistical analysis and characterization, A.M.A. contributed finance assistance towards characterizations and reagents, A.A.B. performed data analysis and contributed resources, N.Y.I. performed experiment and data analysis and sourced for references, and E.A.O. conceived the work, and supervised it.

Funding

This study was funded by Deanship of Scientific research, Northern Border University, Saudi Arabia, for supporting this work through project number "NBU-FFR-2025-2985-07" and also by Princess Nourah bint Abdulrahman University Researchers Supporting Project number (PNURSP2025R65), Princess Nourah bint Abdulrahman University, Saudi Arabia.

Declarations

Competing interests

The authors declare no competing interests.

Additional information

Correspondence and requests for materials should be addressed to A.M.B.